Draft version April 28, 2006
Preprint typeset using LaTeX style emulateapj v. 9/08/03

THE H I CONTENT OF E+A GALAXIES

P. Buyle[1], D. Michielsen[2], S. De Rijcke[1,5], D.J. Pisano[3,6], H. Dejonghe[1], K. Freeman[4]

Draft version April 28, 2006

ABSTRACT

We present deep single-dish H I observations of a sample of six nearby E+A galaxies ($0.05 < z < 0.1$). A non-negligible fraction of a local sample of E+As are detected in HI. In four galaxies, we have detected up to a few times 10^9 $M_\odot$ of neutral gas. These E+A galaxies are almost as gas-rich as spiral galaxies with comparable luminosities. There appears to exist no direct correlation between the amount of H I present in an E+A galaxy and its star-formation rate as traced by radio continuum emission. Moreover, the end of the starburst does not necessarily require the complete exhaustion of the neutral gas reservoir. Most likely, an intense burst of star formation consumed the dense molecular clouds, which are the sites of massive star formation. This effectively stops star formation, even though copious amounts of diffuse neutral gas remain. The remaining H I reservoir may eventually lead to further episodes of star formation. This may indicate that some E+As are observed in the inactive phase of the star-formation duty cycle.

Subject headings: galaxies: evolution, galaxies: elliptical, galaxies: ISM, galaxies: fundamental parameters

1. INTRODUCTION

At $z \approx 0.5$, galaxy clusters contain a population of blue, distorted galaxies that is missing in local clusters: the so-called Butcher-Oemler effect (Butcher & Oemler 1978). In their spectroscopic study of blue galaxies in three clusters at z∼0.31 Couch & Sharples (1987) found that sixty percent of these blue galaxies (classified as Type 3 galaxies) have optical spectra characterised by strong Balmer absorption lines, typical for a very young stellar population, but with weak, if any, emission lines, such as [O II] λ3727Å. Since these spectra are a superposition of an old stellar population, resembling that of an elliptical 'or E' galaxy, and a young stellar population, dominated by A stars, these galaxies are called E+A galaxies. In the notation of Dressler et al. (1999), these galaxies would be classified as k+a/a+k, satisfying the criteria EW([O II])< 5Å and EW(Hδ) >3Å. While at $z \approx 0.4$, about 20% of all cluster galaxies are classified as E+As (Belloni et al. 1995), they constitute less than 1% of the present-day clusterpopulation (Fabricant et al. 1991).

Apparently, these galaxies are observed during a quiescent phase, which explains the lack of emission lines, soon after a vigorous starburst, which explains the strong Balmer absorption lines. Due to the short lifetimes of the stars causing the Balmer absorption, the starburst must have ended no more than ~ 1 Gyr ago (Dressler & Gunn 1983; Poggianti et al. 1999). E+As often have disturbed morphologies, e.g. tidal tails, suggestive of recent merger or interaction events. They span the whole morphological range, from bulge-dominated with underlying disks to disk-dominated (Tran et al. 2003; Yang et al. 2004). Their high surface brightness sets them apart from the elliptical and lenticular galaxies in the Fundamental Plane. Over time, fading of the stellar population will drive them towards the locus of the E/S0s (Yang et al. 2004; Poggianti et al. 1999). Internal velocity dispersions of galaxies classified as E+As appear to increase as a function of redshift, going from $\sigma \simeq 150$ km s^{-1} at $z = 0.3$ to $\sigma \simeq 250$ km s^{-1} at $z = 0.83$ (Tran et al. 2003). This trend suggests that massive galaxies undergo an E+A phase, i.e. are observed in a post-starburst phase, at earlier cosmic times than less massive ones. This is reminiscent of the "down-sizing" phenomenon in star-forming galaxies (Cowie et al. 1996), according to which the masses of galaxies hosting star formation decrease as the Universe ages.

Although the majority of low-z E+A galaxies have a smooth light distribution, many of them also show slightly disturbed morphologies (e.g. warps and dust lanes). Based on this, Zabludoff et al. (1996) argued that the E+A phase is the aftermath of a vigorous starburst, triggered by a major merger or interaction. This is corroborated by a study of E+A galaxies drawn from the 2dFGRS catalogue (Blake et al. 2004). About three quarters of all E+A galaxies are found in the field (i.e. outside clusters), simply because most of the galaxies in the universe do not reside in clusters. However, the *fraction* of E+As is four times higher in clusters than in the field (Zabludoff et al. 1996; Tran et al. 2004). The spatial distribution of E+A galaxies in clusters is more extended than that of quiescent galaxies, but less extended than that of emission-line galaxies (Dressler et al. 1999), suggesting that processes such as galaxy harassment or ram-pressure stripping, which are specific to clusters, can also cause the E+A phenomenon. Based on the 2dFGRS E+A sample, Blake et al. (2004) find that the distribution of *local* environments of E+A galaxies closely traces that of the ensemble of 2dFGRS galaxies and conclude

[1] Sterrenkundig Observatorium, Universiteit Gent, Krijgslaan 281, S9, B-9000, Ghent, Belgium; Pieter.Buyle@UGent.be, Sven.DeRijcke@UGent.be, Herwig.Dejonghe@UGent.be
[2] School of Physics and Astronomy, University of Nottingham, Nottingham NG7 2RD, UK; dolf.michielsen@nottingham.ac.uk
[3] Naval Research Laboratory, USA; Daniel.Pisano@nrl.navy.mil
[4] Research School of Astronomy and Astrophysics, Australia National University, Cotter Rd, ACT2611, Australia; kcf@mso.anu.edu.au
[5] Post-doctoral Fellow of the Fund for Scientific Research - Flanders, Belgium (F.W.O.)
[6] National Research Council Postdoctoral Fellow

TABLE 1
PROPERTIES OF THE E+A SAMPLE.

Galaxy	RA (J2000)[a] (h,m,s)	δ (J2000)[a] (°,′,″)	M_B (mag)	$v_{\rm hel}$[b] (km s^{-1})	Δv (km s^{-1})	$\int S(v)\,dv$[c] (Jy km s^{-1})	H I mass[b] (10^9 M$_\odot$)
SDSS J210258.87+103300.6	21 02 58.9	+10 33 01	-21.7	27821	440	0.18 ± 0.02	6.5 ± 0.8
SDSS J230743.41+152558.4	23 07 43.4	+15 25 58	-20.4	20894	240	0.04 ± 0.01	0.9 ± 0.3
SDSS J233453.20+145048.7	23 34 53.2	+14 50 49	-20.2	19388	380	0.15 ± 0.02	2.7 ± 0.3c
LCRS B101120.1-024053 (EA17)	10 13 52.4	-02 55 48	-18.2	18258		< 0.18	< 2.9
LCRS B002018.8-415015 (EA18)	00 22 47.1	-41 33 37	-18.9	17941	660	0.15 ± 0.02	2.3 ± 0.3
LCRS B020551.6-453502 (EA19)	02 07 49.7	-45 20 50	-18.9	19186		< 0.07	< 1.2

Galaxy	[OII][d] (Å)	Hδ[d] (Å)	r_e (kpc)	Sérsic index	SFR (M$_\odot$/yr)
SDSS J210258.87+103300.6	-0.68	5.13	4.6	3.2	$10.2^{+15.7}_{-6.5}$
SDSS J230743.41+152558.4	-0.92	6.78	2.0	3.1	$1.2^{+1.8}_{-0.8}$
SDSS J233453.20+145048.7	-1.27	5.18	2.1	3.3	$5.6^{+10.1}_{-3.7}$
LCRS B101120.1-024053 (EA17)	1.68	6.92	1.5	2.7/1.3	$< 8.2^{+18.1}_{-5.9}$
LCRS B002018.8-415015 (EA18)	1.75	5.96	1.7	2.2	$5.3^{+10.4}_{-3.7}$
LCRS B020551.6-453502 (EA19)	0.98	6.08	2.1	1.1	$< 1.8^{+2.7}_{-1.1}$

[a]The coordinates are taken from Goto et al. (2003) in case of the SDSS sample and from Zabludoff et al. (1996) in case of the LCRS sample.
[b]The distance D, required for calculating the HI mass, is estimated as the Hubble distance, $D = v_{\rm hel}/H_0$, with $H_0 = 70$ km s^{-1} Mpc^{-1}.
[c]For the non-detected galaxies, EA17 and EA19, we used a velocity width of 450 km s^{-1}.
[d][OII] and Hδ equivalent widths ($\langle$H$\beta\gamma\delta\rangle$ for the LCRS sample); negative values for [O II] indicate absorption

that whatever causes the E+A phenomenon, must be a very local mechanism, such as encounters of galaxy pairs. This is corroborated by a recent analysis of the environments of E+As selected from the SDSS (Goto 2005).

Most E+As have E/S0-like morphologies, with a small fraction of ongoing interactions. Their luminosity distribution is more similar to the distribution of spectroscopically defined elliptical galaxies than to the luminosity distribution of the ensemble of 2dFGRS galaxies (Blake et al. 2004). However, not all E+As can be associated with mergers and, obviously, more than one evolutionary pathway can lead to a post-starburst galaxy (Tran et al. 2003; Dressler et al. 1999). Numerical simulations show that E+As can indeed be formed via a major merger of two gas-rich spiral galaxies (Bekki et al. 2005). A disk-disk merger event then triggers a starburst, which consumes, or, by feedback, expels most of the available gas and then subsides. The young stars then dominate the optical spectrum for the following few hundred Myr while emission lines are absent. During this time-span, a galaxy would be classified as an E+A. In this case, one expects star-formation to be centrally concentrated, leading to radially decreasing Balmer line strengths (Pracy et al. 2005). Alternatively, star formation can be truncated more or less instantaneously over the whole disk of the galaxy without a starburst, e.g. by the gas being swept away by ram pressure stripping. In this case, as the young star population fades, the older bulge population causes the strengths of the Balmer lines to be radially increasing (Pracy et al. 2005).

The red colours of some Hδ-strong E+As cannot be explained by any plausible starburst model (Couch & Sharples 1987; Blake et al. 2004), leaving heavy dust extinction as the only viable explanation. This hypothesis can be tested by using dust insensitive tracers of star formation. Since radio continuum emission is synchrotron radiation from electrons accelerated in supernova remnants, it is an indirect tracer of star formation. Miller & Owen (2001) observed part of the Zabludoff et al. (1996) sample and detected radio-continuum emission in only two out of fifteen galaxies. Smail et al. (1999) detect five out of eight post-starburst galaxies at radio wavelengths. Radio-continuum observations of a sample of 36 E+As drawn from the SDSS yielded no detections (Goto 2004). If this apparent lack of ongoing star-formation in E+As is true, then no dust obscuration, hiding the star-formation sites, needs to be invoked. Near-infrared studies (Galaz 2000; Balogh et al. 2005) have shown that the u−g and r−k colours, and the Hδ line-strengths of E+As can be well explained by dust-free models in which more than 5% of the stellar mass has recently been produced in a starburst. Hence, the presence of dust is still uncertain because of these contradictory observations.

Up to now only one search for H I in E+As was conducted (Chang et al. 2001). VLA observations of five E+As from the sample of Zabludoff et al. (1996) resulted in the detection of only one field E+A galaxy, EA1, with a total HI mass of $7.1 \pm 0.4 \times 10^9 M_\odot$ (assuming $H_0 = 70$ km s^{-1} Mpc^{-1}). For the four other galaxies, upper lim-

its of order $10^9\,M_\odot$ could be derived. EA1 consists of two components, and is most likely a merger remnant. However, other galaxies in this sample are also optical mergers but they do not contain detectable amounts of gas. We started an H I study of a sample of E+A galaxies in order to constrain the amount of neutral gas present in these systems. In section 2 we describe the sample and the observations. The results are presented in section 3. We discuss these results in section 4 and summarise our conclusions in section 5.

2. OBSERVATIONS

2.1. *The sample*

Since *(i)* the occurrence of the E+A phenomenon seems to be determined predominantly by the local environment, *(ii)* the mechanisms triggering the E+A phenomenon, i.e. mergers, interactions, ram-pressure stripping, act both at high and low redshift, and *(iii)* for a given flux, the H I mass scales with distance squared, we opted to use distance as our main selection criterion to maximise our chances of a detection. We selected the three closest E+A galaxies from the large catalogue compiled by Goto et al. (2003) from the SDSS, and the three closest E+A galaxies from the compilation of Zabludoff et al. (1996). The E+A sample selected from the SDSS by Goto et al. (2003) satisfies very strict criteria and contains only galaxies with EW(Hδ) > 4Å + ΔEW(Hδ), with ΔEW(Hδ) the 1σ error on the Hδ equivalent width, and no detectable [O II] and Hα emission, quantified by the constraints EW([O II]) < ΔEW([O II]) and EW(Hα) < ΔEW(Hα), respectively. The Zabludoff sample satisfies the following criteria: EW(H$\beta\gamma\delta$) > 5.5Å and EW([O II]) < 2.5Å, with EW(H$\beta\gamma\delta$) the mean equivalent width of the Hβ, Hγ, and Hδ absorption lines. Table 1 summarises the properties of the galaxies in our sample.

2.2. *Arecibo observations*

We observed the galaxies SDSS J210258.87+103300.6, SDSS J230743.41+152558.4, and SDSS J233453.20+145048.7 for 7.5 h each, including overhead, with the 305m Arecibo Radio Telescope[7] in Puerto Rico. The observations were scheduled on the nights of 23−25 June, 13−15 July and 28−30 July 2005. Each galaxy was observed for 2.5 hours per day during night-time to minimise solar interference. We used the L-wide receiver which has an average system temperature of $\approx$ 27 K (depending on the elevation of the source). We selected the interim correlator in both linear polarisations to process the data. This resulted in final H I spectra with a total bandwidth of 25 MHz and 12.5 MHz divided over 1024 channels, resulting in a velocity resolution of 6.3 km s^{-1} and 3.15 km s^{-1} respectively. For SDSS J230743.41+152558.4 and SDSS J233453.20+145048.7, we used the radar blanker to minimise the effect of the FAA Airport radar at 1330 MHz and 1350 MHz. The beam size of the L-wide receiver is $3.1' \times 3.5'$. We applied the standard position-switching algorithm. Each galaxy was observed for 5 minutes, followed by a 5 minute offset by $5'$ in right ascension to blank sky, such that we tracked the same azimuth and zenith angle as the on-source scan. This mode was used for all galaxies. We reduced the data by means of the standard Arecibo `IDL` routines, written by P. Perrilat. We calibrated each bandwidth individually and the polarisations were averaged together before a second-order baseline was fit across the interference-free part of the spectrum. We checked, with NED, the recession velocities of all galaxies inside the Arecibo beam to avoid confusion with other objects. The results are presented in section 3.

[7] The Arecibo Observatory is part of the National Astronomy and Ionosphere Center, which is operated by Cornell University under a cooperative agreement with the National Science Foundation.

2.3. *Parkes observations*

We observed the galaxies LCRS B101120.1-024053 (EA17), LCRS B002018.8-415015 (EA18), and LCRS B020551.6-453502 (EA19) with the 64m ATNF Parkes Radio Telescope[8] in Australia from dusk till dawn from 11 till 15 October 2005. EA17 was observed during sunrise. We used the Multibeam Correlator in the MB13 configuration (beam-switching mode) which enabled us to observe with 7 beams simultaneously, with one beam on the source while the other six were pointed adjacently on the sky. The beams were switched in position each 5 minutes. This way, we derived H I spectra with a bandwidth of 64 MHz divided over 1024 channels which yields a spectral resolution of 13.19 km s^{-1} and a beam width of $14.1'$. The integration times, including overhead, were 10 h for EA17, 21 h for EA18, and 10 h for EA19. This resulted in one clear 3σ-detection of EA18. All observational quantities are listed in table 1. The data were reduced by means of the `Livedata` data reduction pipeline, which is especially developed for the Multibeam Correlator. No obvious radio interference could be observed and a second order polynomial was used to fit the spectral baseline, after masking out a region around the optical velocity. Afterwards, all data were combined with the help of the `Gridzilla` software package using the median of the weighted values as an estimator. Finally, residual baseline ripples were removed by using the `mbspect` fitting algorithm in the `MIRIAD` (Sault et al. 1995) software package. Again we checked the recession velocities of all other objects within the Parkes beam to avoid confusion. The results are presented in section 3.

[8] The Parkes telescope is part of the Australia Telescope which is funded by the Commonwealth of Australia for operation as a National Facility managed by CSIRO.

3. RESULTS

3.1. *H I masses*

In Figure 1, we show the H I spectra of our six E+As. Three of them have a clear 3σ detection: SDSS J210258.87+103300.6, SDSS J233453.20+145048.7, and EA18. In the case of SDSS J230743.41+152558.4, there is a peak at the correct velocity, over a velocity width of 240 km s^{-1}, which could be a tentative 2.5σ detection of this galaxy. We did not detect EA17 and EA19. The observations of EA17 were badly affected by solar interference though.

We calculate H I masses for the detected objects and 3σ upper limits for the undetected galaxies using the

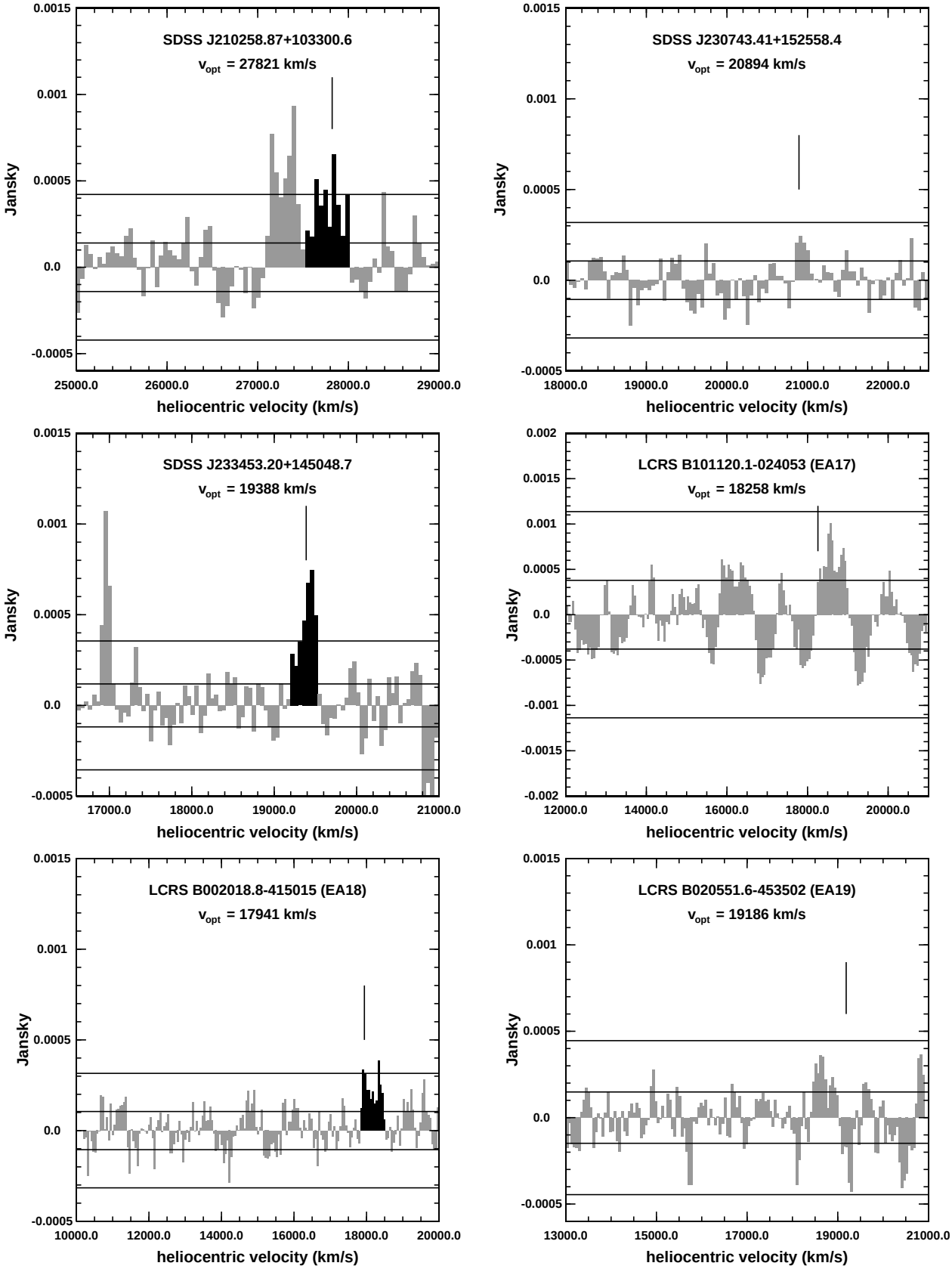

FIG. 1.— The H I spectra of our E+As. The galaxies observed with Arecibo, SDSS J210258.87+103300.6, SDSS J2334543.20+145048.7, SDSS J2330743.41+152558.4, have been rebinned to a velocity resolution of 50 km s^{-1}. The Parkes dataset, LCRS B101120.1-024053 (EA17), LCRS B002018.8-415015 (EA18), LCRS B020551.6-453502 (EA19), has been rebinned to a velocity resolution of 53 km s^{-1}. The name of the galaxy is indicated in each panel along with its optical systemic velocity. The horizontal black lines indicate the -3, -1, 1 and 3 sigma rms noise levels. The vertical black line indicates the optical velocity as found in Goto et al. (2003) and Zabludoff et al. (1996). For the three galaxies with clear detections, the bins corresponding to the galaxy are indicated in black. There is another galaxy within the beam of SDSS J210258.87+103300.6 (the double-horn profile around 27300 km s^{-1}).

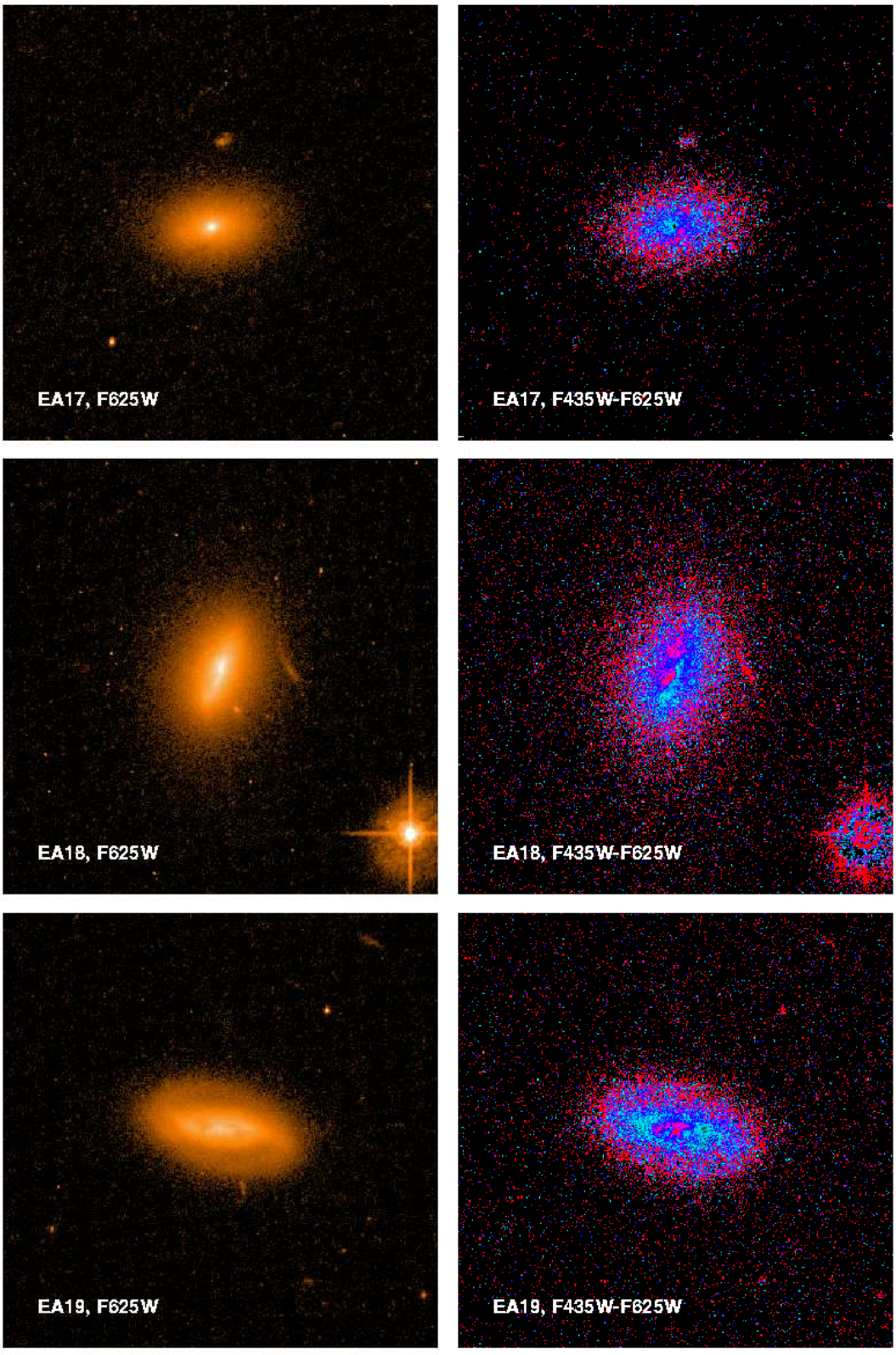

FIG. 2.— Left column: EA17, EA18, and EA19, imaged with ACS using the F625W filter. All galaxies are plotted on the same logarithmic colour scale so their surface brightnesses can be compared directly. Right column: F435W−F625W colour maps of EA17, EA18, and EA19. All galaxies show clear evidence for dust patches and lanes. All galaxies are plotted on the same colour scale, ranging from blue (F435W−F625W= 0.75 mag) to red (F435W−F625W= 1.75 mag). The images measure 25″ on a side.

formula

$$M_{\rm H\,I} = 2.36 \times 10^5\, M_\odot\, D^2 \int S(v)\, dv \qquad (1)$$

with the distance D in Mpc and $\int S(v)\, dv$ the total flux density in Jy km s^{-1}. The distance D was calculated as the Hubble distance $D = v/H_0$, using $H_0 = 70$ km s^{-1} Mpc^{-1}. We find H I masses of $6.5 \pm 0.8 \times 10^9\, M_\odot$ for SDSS J210258.87+103300.6, $0.9 \pm 0.3 \times 10^9\, M_\odot$ for SDSS J230743.41+152558.4, $2.7 \pm 0.3 \times 10^9\, M_\odot$ for SDSS J233453.20+145048.7, and $2.3 \pm 0.3 \times 10^9\, M_\odot$ for EA18, as listed in Table 1. To estimate the error on the H I mass of a galaxy, we generated 50000 statistically equivalent renditions of its radio spectrum by adding Gaussian noise to the original spectrum, using the measured 1σ noise on the original datapoints. The mass error is taken to be the rms of the 50000 masses measured from these spectra. The 3σ upperlimits for the gas content of EA17 and EA19 are $2.9 \times 10^9\, M_\odot$ and $1.2 \times 10^9\, M_\odot$ respectively, assuming a total velocity width of 450 km s^{-1} (the average velocity width of the detected galaxies).

3.2. *Dust content*

Given the small angular sizes of these galaxies, their dust content can only be studied accurately with the supreme spatial resolution of the Hubble Space Telescope (HST). The HST archive contains images of EA17, EA18, and EA19, obtained with the Advanced Camera for Surveys (ACS) through the F435W and F625W filters. In Fig. 2, we show the F625W images and F425W−F625W color maps of these galaxies. From the images it is obvious that the E+A class of galaxies comprises very different morphological types.

EA17 has a smooth appearance, but it also contains a dust lane, which is clearly visible in both the colour-map and plain image. The only galaxy of this sample of three, that was detected in H I, is EA18, which is an irregular-looking galaxy with lots of red and blue patches along the major axis, pointing to dust and/or young stars. EA18 appears also to be warped. Finally, EA19 is a spiral (Sab) galaxy, with two spiral arms nicely visible in both images. The spiral arms are slightly bluer than the rest of the disk and the centre contains blue and red patches, pointing again to dust and/or young stars.

From just this small sample, it is already clear that dust is present near the centres of some E+A galaxies. Along with the presence of neutral H I gas this might indicate that on-going star formation could in fact be hidden by dust.

3.3. *Environment*

Although E+A galaxies are predominately located in the field (i.e. outside clusters), their fraction is four times higher in clusters (Zabludoff et al. 1996; Tran et al. 2004). By investigating their spatial distribution inside clusters, Dressler et al. (1999) showed that an E+A phenomenon can be caused by environmental processes such as galaxy harassment or ram-pressure stripping. Such processes act mostly on the neutral hydrogen content of galaxies and can therefore be investigated by means of our observations.

We adopted the determination of cluster membership of Zabludoff et al. (1996) and also checked the number of neighbours within a radius of 0.5Mpc of each galaxy. Those E+As that were listed in Zabludoff et al. (1996) as being cluster members (EA4 and EA11) have more than 10 known neighbours. Others, such as EA1, EA3, EA18 have 1 or 2 known neighbours and are clearly field galaxies, while the remaining ones have 3-7 known neighbours. For the SDSS galaxies from Goto et al. (2003), cluster membership is not given. Based on the number of known near neighbours, only SDSS J230743.41+152558.4 is a possible cluster galaxy.

Hence, of the five E+As detected at 21 cm up to now, one is a cluster member (SDSS J230743.41+152558.4) and four are not. Of those not detected, two are cluster members and four are not. From this result, it is clear that it is premature to draw conclusions on the environment by means of neutral hydrogen observations. In order to do so, a larger sample is required.

Table 2
Properties of the E+A galaxies of Chang et al. (2001).

Galaxy	[O II]^a (Å)	Hδ^a (Å)	H I mass^b (10^9 M$_\odot$)
EA01	1.80	8.98	7.1
EA02	1.25	7.98	< 3.1
EA03	-0.29	8.13	< 3.9
EA04	1.37	9.82	< 2.0
EA11	2.16	6.96	< 4.7

[a] [O II] and Hδ equivalent widths ($\langle$H$\beta\gamma\delta\rangle$); negative values for [O II] indicate absorption

[b] The distance D, required for calculating the HI mass, is estimated as the Hubble distance, $D = v_{\rm hel}/H_0$, with $H_0 = 70$ km s^{-1} Mpc^{-1}.

3.4. *Optical emission line strengths*

As E+A galaxies are defined by means of their optical spectra, and more precisely by the equivalent widths of primarily the emission lines [O II]and Hδ (Zabludoff et al. 1996; Goto et al. 2003), one can investigate any trend between the neutral hydrogen content and the equivalents widths. For our sample we list these values in Table 1. We restate that our E+A galaxies are compiled from two different samples with each different constraints concerning the equivalent widths of [O II] and Hδ. In Table 2 we list the EW([O II]) and EW(Hδ) for the undetected galaxies from Chang et al. (2001).

Both groups of detected and undetected E+A galaxies at 21 cm contain a mixture of [O II] absorption and emission lines. Similarly, E+A galaxies with low and high EW(Hδ) are detected. We conclude that again a larger sample is needed in order to investigate any trend between the optical emission lines and their neutral hydrogen content.

3.5. *Star-formation rate*

We estimate the star-formation rate (SFR) associated with the observed HI masses using the relation

$$\Sigma_{\rm SFR} \approx 2.5^{\pm 0.7} \times 10^{-10} \left(\frac{\Sigma_{\rm gas}}{M_\odot\, {\rm pc}^{-2}} \right)^{1.40^{\pm 0.15}} M_\odot\, {\rm pc}^{-2}\, {\rm yr}^{-1}, \qquad (2)$$

(Kennicutt 1998). We substituted the total HI mass divided by πR_e^2, with R_e the half-light radius, for the gas surface density Σ_{gas}. From the archival F625W HST/ACS images of EA17, EA18 and EA19, we derived surface brightness profiles as a function of radius by integrating the light in circular apertures centered on the galaxy. A similar method was applied to derive the half-light radii for the SDSS galaxies from Sloan r-band images. We fitted seeing or PSF convolved Sérsic profiles to the surface brightness profiles of all galaxies. The seeing and PSF profiles are determined from about 10 stars in each image. We used the surface brightness profile of a galaxy, extrapolated beyond the last data point by the best fitting Sérsic profile, to measure the half-light radii of these E+As. The SFR surface density, Σ_{SFR}, was then converted into a global SFR by multiplying with πR_e^2. In all cases but SDSS J230743.41+152558.4 and EA19, we found the E+As detected at 21 cm to have SFRs in the range $5 - 10\,M_\odot\,\mathrm{yr}^{-1}$ (see Table 1), which is higher than expected for post-starburst galaxies. Hence, these gas-rich E+As could be actively forming stars at quite high rates but the star-formation sites are obscured by dust. Alternatively, although much gas is present, almost no stars are being formed. The radio continuum observations of Miller & Owen (2001) rule out star formation at a rate higher than $1.0 - 1.5\,M_\odot\,\mathrm{yr}^{-1}$ in the case of EA17 and EA18. These authors measure a star formation rate of $1.5\,M_\odot\,\mathrm{yr}^{-1}$ in EA19. While the star formation rate of EA19 agrees roughly with our upper limit, the high star formation rates of EA17 and EA18 derived from their HI content are in clear contradiction with the very low rates derived from radio continuum observations. Unfortunately, no radio continuum observations have been performed of SDSS J210258.87+103300.6, SDSS J230743.41+152558.4, and SDSS J233453.20+145048.7 so far.

4. DISCUSSION

Three out of the six galaxies observed by us contain detectable amounts of neutral gas and one is a border case. Both the SDSS and the Zabludoff samples satisfy very strict selection criteria and surely do not show any optical evidence for star formation: these appear to be true post-starburst galaxies. They do, however, contain significant amounts of neutral gas. EA19 is not detected by us in 21 cm line emission, with a 3σ upperlimit on the H I mass of $1.2 \times 10^9\,M_\odot$. EA18 was detected by us, with a 21 cm flux consistent with an H I mass of $2.3 \pm 0.3 \times 10^9\,M_\odot$ of H I.

In Fig. 3, we plotted $\log(M_{HI}/L_B)$ versus $\log(L_B)$, L_B the B-band luminosity expressed in solar B-band luminosities, for a sample of spiral galaxies (Helmboldt et al. 2004), elliptical galaxies (Georgakakis et al. 2001), and E+A galaxies (this work and Chang et al. 2001) along with the predicted $\log(M_{HI}/L_B)$ versus $\log(L_B)$ relation for late-type galaxies (Nagashima & Yoshii 2004). For the E+As from the SDSS sample, we converted the SDSS g and r magnitudes to the B-band magnitude using the conversion formulae of Jester et al. (2005). The b_J magnitudes of the LCRS E+As were converted into B-band magnitudes using the relation $m_B = m_J + 0.28(\mathrm{B-V})$ from Maddox, Efstathiou, Sutherland (1990). Using the mean B−V colour of the SDSS E+As, $\langle(\mathrm{B-V})\rangle = 0.78$ mag, in this equation, we find $m_B \approx m_J + 0.22$ mag. The absolute B-band magnitudes found by applying these conversion formulae are also listed in Table 1. Ellipticals with young spectroscopic ages ($\lesssim 1 - 2$ Gyr) are generally more gas-rich than older elliptical galaxies, which Georgakakis et al. (2001) interpret as evidence for a merger origin for elliptical galaxies: the starburst following the merger rapidly consumes the gas reservoir and subsequent quiescent star formation consumes the gas at a much slower rate. It should be noted that Georgakakis et al. (2001) include only ellipticals brighter than $M_B = -18.5$ mag, or $\log(L_B) = 9.5$, in their sample because fainter galaxies are likely to have experienced different evolutionary histories. The resulting sample of ellipticals spans about the same luminosity range as the E+A samples.

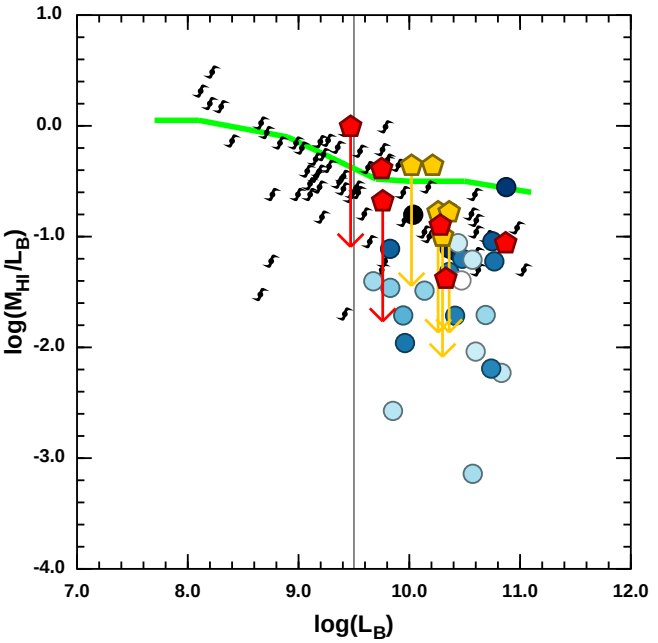

FIG. 3.— $\log(M_{HI}/L_B)$ versus $\log(L_B)$. Spiral galaxies (Helmboldt et al. 2004) are depicted by spiral symbols, elliptical galaxies (Georgakakis et al. 2001) by blue circles (the shade of blue is an indication of spectroscopic age and the vertical black line shows the luminosity limit of $\log(L_B)$=9.5 that was used by Georgakakis et al. (2001)), and E+A galaxies by red circles (this work) and orange circles (Chang et al. 2001). The predicted trend for late-type galaxies by the semi-analytical models of Nagashima & Yoshii (2004) is plotted in green.

As is clear from Fig. 3, some E+As are more gas-rich than most young elliptical galaxies. This is most likely not a selection effect, since the E+A data set was assembled based on optical, spectral properties and the elliptical galaxies were selected according to optical morphological considerations, not on HI mass. One would, moreover, expect the Georgakakis et al. (2001) data set to be complete for galaxies with large HI masses. We performed a Kolmogorov-Smirnov (KS) and Wilcoxon (W) test on the $\log(M_{HI}/L_B)$ distribution (within the same magnitude limits, both in L_B and $\log(M_{HI}/L_B)$, i.e. in the region defined by the detected E+As) and found that the distribution of E+A galaxies (i) corresponds with that of spiral and young elliptical galaxies with a significance of respectively 99% (KS) or 94% (W) and 65% (KS) or 79% (W) and (ii) differs from that of

old elliptical galaxies with a confidence level of 79% (KS) or 78% (W). This statistical test and Fig. 3 might suggest a gas depletion time sequence, with E+As being observed less than ~ 500 Myr after the termination of the starburst that followed the putative merger (Yang et al. 2004), young ellipticals after $\lesssim 1-2$ Gyr, and old ellipticals at later times. However, one should note that the difference between the distributions of E+As and elliptical galaxies has just a significance of 1σ. In order to derive conclusive evidence for this suggestion, a larger statistical sample of HI masses and spectroscopic ages of E+As is essential. Nevertheless, if correct, this ties together with the morphological study of 5 E+As from the Zabludoff (1996) sample with HST by Yang et al. (2004), who suggest that E+As are likely to evolve to elliptical galaxies with power-law density profiles.

One should also note that the end of a starburst does not necessarily require the complete exhaustion of the neutral gas reservoir. This could be explained by the fact that neutral gas itself is not the raw material for star formation: stars form in the dense cores of molecular clouds. Kohno et al. (2002) have obtained CO($1 \rightarrow 0$) and HCN($1 \rightarrow 0$) observations of the nearby post-starburst galaxy NGC5195, which, interestingly, forms an interacting pair with NGC5194. These authors note a central decrease of the mass fraction of dense molecular cores, leaving only diffuse molecular gas, evidenced by a very low central $L_{\rm HCN}/L_{\rm CO}$ value. Most likely, an intense central burst of star formation ~ 1 Gyr ago, responsible for the observed population of A stars, evaporated the dense molecular clouds, which are the sites where massive stars form. This effectively stopped further star formation, although large amounts of diffuse neutral and molecular gas remain. A similar mechanism may be responsible for switching off the starburst in E+A galaxies without the necessity of consuming the complete gas reservoir. The remaining H I reservoir in some E+As may eventually lead, after gas has been allowed to condense into molecular cores, to further episodes of star formation. Eq. (2), which is based on observations of normal spiral galaxies that host a balanced mix of neutral and molecular gas, may therefore not be applicable to post-starburst galaxies.

5. CONCLUSIONS

We present deep single-dish H I observations of a sample of six nearby E+A galaxies ($0.05 < z < 0.1$). We find H I masses of $6.5 \pm 0.8 \times 10^9\,M_\odot$ for SDSS J210258.87+103300.6, $0.9 \pm 0.3 \times 10^9\,M_\odot$ for SDSS J230743.41+152558.4, $2.7 \pm 0.3 \times 10^9\,M_\odot$ for SDSS J233453.20+145048.7, and $2.3 \pm 0.3 \times 10^9\,M_\odot$ for EA18. The 3σ upperlimits for the gas content of EA17 and EA19 are $2.9 \times 10^9\,M_\odot$ and $1.2 \times 10^9\,M_\odot$ respectively, assuming a total velocity width of 450 km s^{-1} (the average velocity width of the detected galaxies). The three galaxies from the SDSS sample satisfy very strict selection criteria and, for all practical purposes, can be considered to be truly post-starburst galaxies.

The E+A galaxies detected in 21 cm line emission are almost as gas-rich as spiral galaxies with comparable luminosities. By plotting these E+As, spiral galaxies, and elliptical galaxies in a $\log(M_{\rm HI}/L_B)$ versus $\log(L_B)$ diagram, and performing a Kolmogorov-Smirnov and Wilcoxon test we suggest that existence of a gas depletion time sequence, with E+As being observed very shortly after the termination of the starburst that ensued from the putative merger, young ellipticals after $\lesssim 1-2$ Gyr, and old ellipticals at even later times. This would tie together with the morphological study of 5 E+As from the Zabludoff (1996) sample with HST by Yang et al. (2004), who suggest that E+As are likely to evolve to elliptical galaxies with power-law density profiles. However, the conclusions drawn here are just based on 1σ trends. A larger sample of H I detections and spectroscopic ages of E+As is required to investigate this hypothesis.

The presence of H I in an E+A galaxy can be explained in two ways.
(i) We can interpret the lack of on-going star-formation in E+A galaxies, suggested by previous radio continuum observations (Miller & Owen 2001) and indirectly by their selection criteria, and the fact that the end of the starburst does not necessarily require the complete exhaustion of the neutral gas reservoir, as being due to the effect the starburst has on the dense molecular cores which are responsible for the massive star formation. An intense burst of star formation can evaporate the dense molecular clouds, effectively stopping further star formation, even though copious amounts of diffuse neutral and molecular gas remain. The remaining H I reservoir in some E+As may eventually lead, after the gas has again condensed into molecular cores, to further episodes of star formation. This may indicate that E+As are observed in the inactive phase of the star-formation duty cycle.
(ii) A second possibility is what previously has been proposed by Couch & Sharples (1987) and Blake et al. (2004). There might still be on-going star-formation associated with the presence of H I gas, which is hinted from the high SFR (see Table 1) of our E+A galaxies; however it cannot be observed since it is obscured by dust (Smail et al. 1999), which is suggested by the ACS images in Fig. 2, and/or optical emission lines might be a poor way of isolating true post-starbust systems. In this case E+A galaxies are in the active star-formation phase and will presumably exhaust all their gas content.

PB acknowledges financial support from the Bijzonder OnderzoeksFonds (BOF). DM is supported by the MAGPOP EU Marie Curie Training and Research Network. SD acknowledges financial support from the Fonds voor Wetenschappelijk Onderzoek – Vlaanderen (FWO). This research was performed while D. J. P. held a National Research Council Research Associateship Award at the Naval Research Laboratory. Basic research in astronomy at the Naval Research Laboratory is funded by the Office of Naval Research. This work has made use of the NASA/IPAC Extragalactic Database (NED) which is operated by the Jet Propulsion Laboratory, California Institute of Technology, under contract with the National Aeronautics and Space Administration. Based on observations made with the NASA/ESA Hubble Space Telescope, obtained from the data archive at the Space Telescope Institute. STScI is operated by the association of Universities for Research in Astronomy, Inc. under the NASA contract NAS 5-26555.

REFERENCES

Balogh, M. L., Miller, C., Nichol, R., Zabludoff, A., & Goto, T. 2005, MNRAS, 360, 587
Bekki, K., Couch, W. J., Shioya, Y., & Vazdekis, A. 2005, MNRAS, 359, 949
Belloni, P., Bruzual, A. G., Thimm, G. J., Roser, H.-J., 1995, A&A, 297, 61
Blake, C., Pracy, M. B., Couch, W. J., Kenji, B., Lewis, I., Glazebrook, K., Baldry, I. K., Baugh, b. M., Bland-Hawthorn, J., et al., 2004, MNRAS, 355, 713
Butcher, H., Oemler, A., Jr., 1978, ApJ, 219, 18
Chang, T. C., van Gorkum, J. H., Zabludoff, A. I., Zaritsky, D., & Mihos, J. C. 2001, AJ, 121, 1965
Couch, W. J., Sharples, R. M., 1987, MNRAS, 229, 423
Cowie, L. L., Songaila, A., Hu, Ester M., Cohen, J. G., 1996, AJ, 112, 839
Dressler, A., Gunn, J. E., 1983, ApJ, 270, 7
Dressler, A., Smail, I., Poggianti, B. M., Butcher, H., Couch, W. J., Ellis, R. S., & Oemler, A., Jr., 1999, ApJS, 122, 51
Fabricant, D.G., McClintock, J. E., Bautz, M.W., 1991, ApJ, 381, 33
Galaz, G. 2000, AJ, 119, 2118
Georgakakis, A., Hopkins, A. M., Caulton, A., Wiklind, T., Terlevich, A. I., Forbes, D., A., 2001, MNRAS, 326, 1431
Goto, T., Nichol, R. C., Okamura, S., Sekiguchi, M., Miller, C. J., Bernardi, M., Hopkins, A., Tremonti, C., Connolly, A., Castander, F. J., et al. 2003, PASJ, 55, 771
Goto, T. 2004, A&A, 427, 125
Goto, T. 2005, MNRAS, 357, 937
Helmboldt, J. F., Walterbos, R. A. M., bothun, G. D., O'Neil, K., de Blok, W. J. G., 2004, ApJ, 613, 914
Jester, S., Schneider, D. P., Richards, G. T., Green, R. F., Schmidt, M., Hall, P. B., Strauss, M. A., Vanden Berk, D. E., et al., 2005,AJ, 130, 873
Kennicutt, R. C., Jr., 1998, ARA&A, 36, 189
Kohno, K., Tosaki, T., Matsushita, S., Vila-Vilaó, B., Shibatsuka, T., Kawabe, R., 2002, PASJ, 54, 541
Maddox, S. J., Efstathiou, G., Sutherland, W. J., 1990, MNRAS, 246, 433
Miller, N. A., & Owen, F. N. 2001, ApJ, 554, 125
Nagashima, M. & Yoshii, Y., 2004, ApJ, 610, 23
Poggianti, B. M., Smail, I., Dressler, A., Couch, W. J., Barger, J., Butcher, H., Ellis, E. S., & Oemler, A., Jr., 1999, ApJ, 518, 576
Pracy, M. B., Couch, W. J., Blake, C., Bekki, K., Harrison, C., Colless, M., Kuntschner, H., & de Propris, R. 2005, MNRAS, 359, 1421
Sault, R.J., Teuben, P.J. & Wright, M.C.H., 1995, in Shaw R., Payne H.E., Hayes, J.J.E., eds, ASP Conf Ser. Vol. 77, Astronomical Data Analysis Software and Systems IV. Astron. Soc. Pac., San Fransisco, p. 433 2005, MNRAS, 359, 1421
Smail, I., Morrison, G., Gray, M. E., Owen, F. N., Ivison, R. J., Kneib, J.-P., Ellis, R. S Gray, M. E., et al. 1999, ApJ, 525, 609
Tran, K.-V. H., Franx, M., Illingworth, G., Kelson, D. D., & van Dokkum, P. 2003, ApJ, 599, 865
Tran, K.-V. H., Franx, M., Illingworth, G. D., van Dokkum, P., Kelson, D. D., & Magee, D. 2004, ApJ, 609, 683
Yang, Y., Zabludoff, A. I., Zaritsky, D., Lauer, T. R., & Mihos, J. C. 2004, ApJ, 607, 258
Zabludoff, A. I., Zaritsky, D., Lin, H., Tucker, D., Hashimoto, Y., Shectman, S. A., Oemler, A., & Kirshner, R. P. 1996, ApJ, 466, 104